Monthly Notices
of the
ROYAL ASTRONOMICAL SOCIETY

Mon. Not. R. Astron. Soc. **420,** 1481–1494 (2012) doi:10.1111/j.1365-2966.2011.20135.x

The importance of the local density in shaping the galaxy stellar mass functions⋆

Benedetta Vulcani,[1,2]† Bianca M. Poggianti,[2] Giovanni Fasano,[2] Vandana Desai,[3] Alan Dressler,[4] August Oemler, Jr,[4] Rosa Calvi,[1] Mauro D'Onofrio[1] and Alessia Moretti[1,2]

[1]*Department of Astronomy, Padova University, Vicolo Osservatorio 3, I-35122 Padova, Italy*
[2]*INAF-Astronomical Observatory of Padova, Vicolo Osservatorio 5, I-35122 Padova, Italy*
[3]*Spitzer Science Center, California Institute of Technology, Pasadena, CA 91125, USA*
[4]*Carnegie Observatories, 813 Santa Barbara Street, Pasadena, CA 91101-1292, USA*

Accepted 2011 November 3. Received 2011 November 3; in original form 2011 July 26

ABSTRACT

Exploiting the capabilities of four different surveys – the Padova–Millennium Galaxy and Group Catalogue (PM2GC), the WIde-field Nearby Galaxy-cluster Survey (WINGS), the IMACS (Inamori-Magellan Areal Camera and Spectrograph) Cluster Building Survey (ICBS) and the ESO (European Southern Observatory) Distant Cluster Survey (EDisCS) – we analyse the galaxy stellar mass distribution as a function of local density in mass-limited samples, in the field and in clusters from low ($z \geq 0.04$) to high ($z \leq 0.8$) redshift. We find that at all redshifts and in all environments, local density plays a role in shaping the mass distribution. In the field, it regulates the shape of the mass function at any mass above the mass limits. In clusters, it seems to be important only at low masses ($\log M_*/\mathrm{M}_\odot \leq 10.1$ in WINGS and $\log M_*/\mathrm{M}_\odot \leq 10.4$ in EDisCS), otherwise it seems not to influence the mass distribution. Putting together our results with those of Calvi et al. and Vulcani et al. for the global environment, we argue that at least at $z \leq 0.8$ local density is more important than global environment in determining the galaxy stellar mass distribution, suggesting that galaxy properties are not much dependent on halo mass, but do depend on local scale processes.

Key words: galaxies: clusters: general – galaxies: evolution – galaxies: formation – galaxies: fundamental parameters – galaxies: luminosity function, mass function.

1 INTRODUCTION

It is well known that galaxies reside in environments that span a wide range of galaxy densities (number of galaxies per Mpc^3). Many authors have shown that galaxy density plays an important role in determining many galaxy properties, such as star formation rate, rest-frame colours, gas content and morphology (see e.g. Dressler 1980; Kauffmann et al. 2004; Baldry et al. 2006; Ellison et al. 2009). Hence, if we wish to understand the physical processes that drive galaxy evolution, we have to test for systematic differences between galaxies in various environments.

In addition, it is equally well known that galaxies are characterized by a wide range of total stellar masses. Several works have shown that mass is a crucial parameter in driving galaxy evolution and have claimed that in some cases mass plays a more important role than the environment in influencing galaxy properties (see e.g. Peng et al. 2010; Grützbauch et al. 2011a). We note that to fully characterize the importance of the mass, it would be very interesting and important to have the total galaxy mass (dark+luminous), but that is observationally challenging to achieve. Hence, all of the cited studies in this paper investigate only the galaxy stellar mass, as tracer of the luminous galaxy matter. Among others, Kauffmann et al. (2004) have shown that at low-z, at fixed stellar mass, there is nearly no dependence of structural properties like Sersic index or concentration parameter on local galaxy density. Baldry et al. (2006) have found that the colour–mass and colour–concentration index relations do not depend strongly on environment, while the fraction of galaxies on the red sequence depends strongly on both stellar mass and environment. Mouhcine, Baldry & Bamford (2007) have found no dependence of the relationship between galaxy stellar mass and gas-phase oxygen abundance on local galaxy density. At higher redshifts in zCOSMOS, Scodeggio et al. (2009) observed a significant mass and optical colour segregation, in the sense that the

⋆This paper includes data gathered with the 6.5-m Magellan Telescopes located at Las Campanas Observatory, Chile.
†E-mail: benedetta.vulcani@oapd.inaf.it

© 2011 The Authors
Monthly Notices of the Royal Astronomical Society © 2011 RAS

median value of the mass distribution is larger and the rest-frame optical colour is redder in regions of high galaxy density. However, considering only galaxies in a narrow range of stellar mass, they no longer observed any significant colour segregation with density.

Trying to disentangle the contribution of the environment and mass on the evolution, in order to quantify separately their importance, has been the aim of several works. Studies by van der Wel (2008) showed that morphology and structure are intrinsically different galaxy properties, and that they depend differently on galaxy mass and environment. Structure mainly depends on galaxy mass whereas morphology mainly depends on environment. Grützbauch et al. (2011a) found that galaxy colour and the fraction of blue galaxies depends very strongly on stellar mass at $0.4 < z < 1$, while there is only a weak dependence on local density. This environmental influence is most visible in the colours of intermediate-mass galaxies ($10.5 < \log M_*/\mathrm{M}_\odot < 11$), whereas colours of lower- and higher mass galaxies remain largely unchanged with redshift and environment. Fixing the stellar mass, the colour–density relation almost disappears, while the colour–stellar mass relation is present at all local densities. They also found a weak correlation between stellar mass and environment at intermediate redshifts. Restricting their analysis to a subsample of red galaxies, Moresco et al. (2010) also found that the colour distribution is not strongly dependent on environment for all mass ranges, exhibiting only a weak trend such that galaxies in overdense regions are redder than galaxies in underdense regions. On the other hand, the dependence on mass is far more significant, with the average colours of massive galaxies being redder than low-mass galaxies. Grützbauch et al. (2011b) found that galaxy colour strongly correlates with stellar mass, but it does not with local density at fixed mass at all redshifts up to $z \sim 3$.

Since mass and environment may also be strictly linked, it is important to know how one depends on the other and in particular to understand whether the stellar mass distribution, usually regarded as an intrinsic property of a galaxy, can be influenced by the environment, being tightly coupled for example to the depth of the halo potential and thus the halo mass. Massive elliptical galaxies are often found in the cores of galaxy clusters, or at high local densities, while lower mass spirals are preferentially located in the outskirts of large structures or in small groups. However, massive ellipticals are also found in the field (e.g. Colbert, Mulchaey & Zabludoff 2001), and low-mass galaxies with elliptical morphology are found preferentially at high local densities (e.g. Roberts et al. 2007).

Overall, it is still not fully clear how a galaxy's stellar mass depends on the environment and how this dependence evolves with redshift.

The distribution of galaxy stellar masses is also of fundamental importance for studying the assembly of galaxies over cosmic time. Establishing whether the environment can regulate the mass distribution could add an important piece in the puzzle of galaxy evolution, clarifying the relation between these two quantities. Both estimating galaxy masses and defining and characterizing the environment have their own uncertainties and limitations. Furthermore, all the mass estimates are strictly linked to the adopted initial mass function (IMF). It is implicitly assumed that the IMF is universal, but it could be different for galaxies of all types (see e.g. Gunawardhana et al. 2011). Moreover, the stellar mass can be model dependent (see Maraston 2005 versus Bruzual & Charlot 2003 models) and again the choice of the model affects differently galaxies of different ages/metallicities. Results of different models can be controversial and lead to different findings. As a consequence, mass estimates are subject to systematic uncertainties (due also to star formation history and metallicity variations) that are of the order of at least a factor 2 or more.

As far as the environment is concerned, definitions used to properly characterize it are mostly arbitrary. First of all, we have to distinguish between global and local environment: in the first case, according to the host halo mass, galaxies are commonly subdivided into e.g. superclusters, clusters, groups, field galaxies, voids, while in the second case environment is described through the estimates of the local density, which can be parametrized in several ways, following different techniques. For example, it is possible to fix the metric aperture in which the number of neighbours of a galaxy are counted or to measure the distance to the nth nearest neighbour (with n typically in the range of 5–10). Even if there is a sort of general correlation between global and local environments, as we will show also in this paper, the two definitions of environments are not at all equivalent (Muldrew et al. 2011).

Focusing on local environment, galaxy densities also critically depend on how the sample is selected: adopting a magnitude-limited or a mass-limited sample entails a different selection of galaxies involved in the estimates of local density and hence results can strongly change, according to the selection choices and the limits adopted (see e.g. Wolf et al. 2009; Haas, Schaye & Jeeson-Daniel 2012).

No matter how local density is parametrized, the variation of the galaxy stellar mass distribution in regions of different density has been observed for mass-limited samples both in the local Universe (see e.g. Kauffmann et al. 2004; Baldry et al. 2006) and at higher redshifts (see e.g. Bundy et al. 2006; Scoville et al. 2007; Scodeggio et al. 2009; Bolzonella et al. 2010). All the previous studies generally agree in finding that the mass distribution is regulated by local density. Galaxies in lower- and higher density regions show different mass distributions, in the sense that lower density regions are proportionally more populated by lower mass galaxies. However, all of these studies considered a quite wide range of densities and moreover they mainly compared the most extreme environments, to maximize the possible differences. All of them considered general field data, without focusing especially in clusters, while in this paper we make a first attempt to investigate the importance of the local density in regulating the mass distribution in different environments both at low and intermediate redshifts, also considering separately the cluster environment. To do this, we use the Padova–Millennium Galaxy and Group Catalogue (PM2GC) ($0.039 < z < 0.11$; Calvi, Poggianti & Vulcani 2011), the WIde-field Nearby Galaxy-cluster Survey (WINGS) ($0.04 < z < 0.07$; Fasano et al. 2006), the IMACS (Inamori-Magellan Areal Camera and Spectrograph) Cluster Building Survey (ICBS) ($0.25 < z < 0.45$; Oemler et al., in preparation) and the ESO (European Southern Observatory) Distant Cluster Survey (EDisCS) ($0.4 < z < 0.8$; White et al. 2005) data sets.

This paper is organized as follows. In Section 2, we present all the data sets used, describing the galaxy samples. In Section 3.1, we begin our analysis by showing how the mass distribution depends on local density for $z \sim 0$ field galaxies, and in Section 3.2 we focus our attention only on galaxy clusters at similar redshifts. In Section 3.3 we move to higher redshift field galaxies and, finally, in Section 3.4 we show the results for clusters at $0.5 < z < 0.8$. We follow with a discussion in Section 4 and summarize our most important findings in Section 5.

Throughout this paper, we adopt $(H_0, \Omega_\mathrm{m}, \Omega_\lambda) = (70\,\mathrm{km\,s^{-1}\,Mpc^{-1}}, 0.3, 0.7)$ and a Kroupa (2001) IMF, in the range of mass 0.1–100 $\mathrm{M}_\odot$.

2 DATA AND GALAXY SAMPLES

To characterize the mass function in different local density conditions, we take advantage of four different data sets that allow us to analyse galaxies at different redshifts and in different global environments.

In the following, we refer to 'general field' (as in the case of the PM2GC) when we consider a wide portion of the sky, including all environments. In contrast, we refer to 'field' (as in the case of the ICBS) when we start from a cluster survey and we exclude cluster members to consider a non-cluster sample. We need to adopt these definitions given the selection criteria of our surveys (see below).

2.1 PM2GC

To analyse galaxies in the general field in the local Universe we use data from the PM2GC (Calvi et al. 2011), a catalogue of group, binary and single galaxies at $0.03 \leq z \leq 0.11$ drawn from the Millennium Galaxy Catalogue (MGC; Liske et al. 2003), a deep 38-deg^2 *B*-band imaging and optical spectroscopic survey, which provides a high-quality, complete representation of the nearby galaxy populations.

A detailed description of the MGC survey strategy, the photometric and astrometric calibration, the object detection and classification can be found in Liske et al. (2003), while the selection and properties of the galaxy groups are described in Calvi et al. (2011). For this paper, it is worth knowing that the PM2GC spectroscopic sample is essentially complete to $M_B < -18.7$, so there is no need to apply a statistical completeness correction. Absolute *B*-band magnitudes were obtained k-correcting the observed SExtractor 'BEST' magnitudes (MAGAUTO, except in the crowded region where the ISOCOR magnitude was used instead), corrected for Galactic extinction.

In the PM2GC sample, there are 176 groups with at least three members[1] at $0.04 \leq z \leq 0.1$, comprising in total 1057 galaxies, representing 43 per cent of the general field population. The median redshift and velocity dispersion of these groups are $z = 0.0823$ and $\sigma = 192\,\mathrm{km\,s^{-1}}$, respectively. 88 per cent of the groups have fewer than 10 members, and 63 per cent have fewer than five members. Non-group galaxies have been subdivided into 'binary' systems of two bright close companions, and 'single' galaxies with no bright companion within $1500\,\mathrm{km\,s^{-1}}$ and $0.5\ h^{-1}$ Mpc. The binary and single catalogues contain 490 and 1141 galaxies, respectively, at $0.03 \leq z \leq 0.11$. The general field altogether comprises 3210 galaxies at $0.03 \leq z \leq 0.11$ and includes all group, binary and single galaxies as well as other galaxies that belong to groups but are outside each group radial limits or the redshift range for groups.

Stellar masses are taken from Calvi et al. (2011) and were determined using the relation between M/L_B and rest-frame $(B-V)$ colour, following Bell & de Jong (2001) [$\log(M/L_B) = -0.51 + 1.45(B-V)$], and then they were converted to a Kroupa (2001) IMF (for details refer to Calvi et al. 2011). The accuracy of the measured masses is ∼0.2–0.3 dex. As discussed in Calvi et al. (2011), the completeness mass limit for the PM2GC sample is $\log M_*/\mathrm{M}_\odot = 10.25$. Our choice to adopt a mass limit is dictated by the need to ensure completeness, i.e. to include all galaxies more massive than the limit regardless of their colour or type. To determine this limit, we have computed the mass of an object whose observed magnitude is equal to the faint magnitude limit of the survey, and whose colour is the reddest colour of a galaxy at the highest redshift considered. With this selection, we are sure that our results will not be affected for example by the Malmquist bias effect, which leads to the preferential detection of intrinsically bright objects. This effect is instead very important in magnitude-limited samples, where galaxies below a certain brightness are neglected.

The projected local galaxy density is derived from the circular area *A* that, in projection on the sky, encloses the *N* nearest galaxies brighter than an absolute *V* magnitude. The projected density then is $\Sigma = N/A$ in number of galaxies per Mpc^2. For each galaxy in the PM2GC survey, the local galaxy density has been computed from the circular area (A_5) containing the five nearest projected neighbours within $\pm 1000\,\mathrm{km\,s^{-1}}$ from the galaxy and with $M_V \leq -19.85$, which is the *V* absolute magnitude limit at which the sample is spectroscopically complete.

Due to the peculiar geometry of the area covered by the PM2GC survey (a stripe of 0.6×73 deg across the sky), when the local density decreases, the circular area A_5 tends to overflow more and more the survey coverage area, thus producing increasingly unreliable estimates of the local density. To overcome this problem, in measuring local densities we used the photometric and spectroscopic information for all galaxies in the regions of the sky around the MGC ($\pm 1.5^\circ$) from the Sloan Digital Sky Survey (SDSS; York et al. 2000) and the Two degree Field Galaxy Redshift Survey (2dFGRS; Colless et al. 2001), which together yielded a highly complete sample in the regions of interest.

Hereafter, we consider only PM2GC galaxies above the completeness limit $\log M_*/\mathrm{M}_\odot = 10.25$. In this way, our final PM2GC sample consists of 1583 galaxies.

2.2 WINGS

WINGS is a multiwavelength photometric and spectroscopic survey of 77 galaxy clusters at $0.04 < z < 0.07$ (Fasano et al. 2006). Clusters were selected in the X-ray from the *ROSAT* Brightest Cluster sample and its extension (Ebeling et al. 1998, 2000) and the X-ray Brightest Abell-type Cluster sample (Ebeling et al. 1996). WINGS has obtained wide-field optical photometry (*BV*) for all 77 fields (Fasano et al. 2006; Varela et al. 2009), as well as infrared (*JK*) photometry (Valentinuzzi et al. 2009), optical spectroscopy (Cava et al. 2009) and *U*-band (Omizzolo et al., in preparation) for a subset of the WINGS clusters.

For WINGS we consider only spectroscopically confirmed members of 21 clusters. This is the subset of clusters that have a spectroscopic completeness (the ratio of the number of spectra yielding a redshift to the total number of galaxies in the photometric catalogue) higher than 50 per cent. The clusters used in this analysis are listed in Table 1. We apply a statistical correction to account for spectroscopic incompleteness. This is obtained by weighting each galaxy by the inverse of the ratio of the number of spectra yielding a redshift to the total number of galaxies in the photometric catalogue, in bins of 1 mag (Cava et al. 2009).

As for the PM2GC, galaxy stellar masses have been determined using the relation between M/L_B and rest-frame $(B-V)$ colour proposed by Bell & de Jong (2001). The spectroscopic magnitude limit of the WINGS survey is $V = 20$, corresponding to a mass limit of $\log M_*/\mathrm{M}_\odot = 9.8$, above which the sample is unbiased. For a detailed description of the stellar estimates, see Vulcani et al. (2011a).

For each spectroscopically confirmed cluster member in WINGS, the local density has been computed from the circular area (A_{10})

[1] Within these groups a few very massive groups ($\sigma \geq 500\,\mathrm{km\,s^{-1}}$), comparable to clusters, are included (see Calvi et al. 2011).

Table 1. List of WINGS clusters analysed in this paper and their redshift z and velocity dispersion σ.

Cluster name	z	σ (km s^{-1})
A1069	0.0653	690 ± 68
A119	0.0444	862 ± 52
A151	0.0532	760 ± 55
A1631a	0.0461	640 ± 33
A1644	0.0467	1080 ± 54
A2382	0.0641	888 ± 54
A2399	0.0578	712 ± 41
A2415	0.0575	696 ± 51
A3128	0.06	883 ± 41
A3158	0.0593	1086 ± 48
A3266	0.0593	1368 ± 60
A3376	0.0461	779 ± 49
A3395	0.05	790 ± 42
A3490	0.0688	694 ± 52
A3556	0.0479	558 ± 37
A3560	0.0489	710 ± 41
A3809	0.0627	563 ± 40
A500	0.0678	658 ± 48
A754	0.0547	1000 ± 48
A957x	0.0451	710 ± 53
A970	0.0591	764 ± 47

containing the 10 nearest projected neighbours in the photometric catalogue (with or without spectroscopic membership) whose V-band absolute magnitude would be $M_V \leq -19.5$ if they were cluster members. As we only want to count as neighbours the members of the cluster, a statistical correction for field galaxy contamination has been applied to the counts using table 5 in Berta et al. (2006). In particular, since the field counts in the area containing the 10 nearest neighbours are not integer numbers, A_{10} is obtained interpolating the two A_n areas for which the corrected counts (or the number of spectroscopic members, if greater than them) are immediately lower and greater than 10.

A similar interpolation technique has also been used when the circular area containing the 10 nearest neighbours is not fully covered by the available data (galaxies at the edges of the WINGS field). In this case, at increasing n (and the corresponding area A_n), a coverage factor has been evaluated as the ratio between the circular area and the area actually covered by the observations. Then, the counts n have been first multiplied for the corresponding coverage factors and thereafter corrected for the field counts (again always including the spectroscopic members). Finally, as in the previous case, A_{10} has been obtained interpolating the two A_n areas for which the corrected counts are immediately lower and greater than 10.

It is important to stress that the way local density estimates are computed in WINGS and PM2GC is different and, as a consequence, they are not directly comparable. WINGS is not spectroscopically complete, and therefore it is not possible to use a region within ± 1000 km s^{-1} around each galaxy to count all neighbours, as is done in PM2GC. In WINGS, as usually done in clusters, we try to use only cluster members as neighbours adopting a statistical subtraction to remove the interlopers. Moreover, since clusters are highly populated, we can count 10 neighbours around each galaxy.

In contrast, the PM2GC is spectroscopically complete, but a 'membership' to a structure is not meaningful, so we have to define the region to count neighbours adopting a fixed velocity distance. Finally, we use only the fifth neighbour around each galaxy to avoid sampling too large a volume that would include physically distant galaxies in other haloes.

Given the necessarily different criteria for neighbours, it is not possible to compare directly the local density estimates in the two samples.

In WINGS, only galaxies with $\log M_*/\mathrm{M}_\odot \geq 9.8$, lying within $0.6R_{200}$[2] (the largest radius covered approximately in all clusters) are considered. Moreover, brightest cluster galaxies (BCGs) are excluded from our analysis (see Vulcani et al. 2011a for details on the selection criteria). The final WINGS sample consists of 1229 galaxies (1888 once weighted).

2.3 ICBS

The ICBS (Oemler et al., in preparation) is a project focused on the study of galaxy evolution and infall on to clusters from a clustercentric radius $R \sim 5$ Mpc to the cluster regions. Data have been acquired using the wide field of the IMACS on Magellan-Baade.

The ICBS sought to define a homogeneous sample of clusters by selecting the most massive clusters per comoving volume at any redshift. Clusters were selected using the Red-Sequence Cluster Survey (RCS) method Gladders & Yee (2000), either from the RCS itself or from the SDSS in regions of the sky not covered by the RCS. Within each field, galaxies were selected for observations from the RCS or SDSS catalogues, down to a limiting magnitude of $r \approx 22.5$. Spectroscopy of approximately 60 per cent of all objects brighter than this limit was obtained with the IMACS spectrograph on the 6.5-m Baade Telescope at Las Campanas. Of those observed, only about 20 per cent failed to yield redshifts, or turned out to be stars. In addition, broad-band photometry, in either the *BVRI* or *griz* systems, was obtained for each field, either with IMACS or with the wide-field CCD camera on the 2.5-m duPont Telescope.

The data discussed in this paper come from four fields that contain rich galaxy clusters at $z = 0.33, 0.38, 0.42$ and 0.43, as well as other structures at different redshifts. For this sample, we have decided to restrict our analysis to ICBS galaxies in the redshift range of $0.25 < z < 0.45$, in all the environments treated. This was done to focus on a rather limited redshift range in order to use a common mass limit set at $z = 0.45$. We treat separately cluster and field galaxies; hence, we subdivide galaxies into two samples: 'clusters' contain all galaxies within $\pm 3\sigma$ from the cluster redshift, the 'field' include the others.

Since the projected density of cluster/supercluster members is low at large clustercentric distances such as those probed by the ICBS, our sample necessarily includes $\sim$1000 'field' galaxies at a redshift of $0.2 < z < 0.8$ per survey field. The IMACS $f/2$ spectra have an observed-frame resolution of 10 Å full width at half-maximum with a typical signal-to-noise ratio (S/N) $\sim$ 20–30 in the continuum per resolution element.

Details of the data and data analysis are presented in two papers by Oemler et al. (in preparation). Details on absolute magnitudes, mass estimates and completeness weights can be found in Vulcani et al. (2011b). Briefly, absolute magnitudes have been determined using INTERREST (Taylor et al. 2009) from the observed photometry.

[2] R_{200} is defined as the radius delimiting a sphere with interior mean density 200 times the critical density of the Universe at that redshift and is commonly used as an approximation for the cluster virial radius. The R_{200} values for our structures are computed from the velocity dispersions using the formula

$$R_{200} = 1.73 \frac{\sigma}{1000\,(\mathrm{km\,s^{-1}})} \frac{1}{\sqrt{\Omega_\Lambda + \Omega_0(1+z)^3}}\, h^{-1} \quad (\mathrm{Mpc}).$$

When photometry is available, we determine the galaxy stellar mass using the relation between M/L_B and rest-frame $(B-V)$ colour proposed by Bell & de Jong (2001). The error of the measured masses is ∼0.3 dex. As usual, all our masses are scaled to a Kroupa (2001) IMF. Our broad-band photometry does not cover the entire field of our redshift survey. If photometry was not available for a galaxy, synthetic colours were calculated from the flux-calibrated IMACS spectra.

The magnitude completeness limit of the ICBS is $r \sim 22.5$. At our highest ICBS redshift, $z \sim 0.45$, the mass completeness limit is $M_* = 10^{10.5}\,\mathrm{M}_\odot$.

In this paper, galaxies are given weights proportional to the inverse of the spectroscopic incompleteness. Since the main galaxy property we wish to analyse in this work is galaxy stellar mass, the incompleteness correction has been computed taking into account the number of galaxies which have an estimate of the mass (for details, see Vulcani et al. 2011b).

Projected local densities are derived from the rectangular area A that, in projection on the sky, encloses the N nearest galaxies brighter than $r = 22.5$. The projected density is then $\Sigma = N/A$ in number of galaxies per Mpc^2. Densities have been computed separately for cluster and field galaxies and separately for each field. As a consequence, local densities in the different global environments are not directly comparable. In both cases, local incompleteness has been taken into account. For clusters, local densities are derived taking into account all cluster members and estimating the area that encloses the five nearest galaxies. For the field sample, densities are derived considering five nearest galaxies and within the rest-frame velocity dispersion of $\pm 1000\,\mathrm{km\,s^{-1}}$. Due to the relatively small size of our fields, it has not been possible to find any companion within $\pm 1000\,\mathrm{km\,s^{-1}}$ for some field galaxies. They are a 'very isolated sample' and we gave to them a very low value of local density, so that they will be included in the lowest local density bin.

In the cluster sample, we exclude BCGs, whose properties could alter the general trends, and consider all members regardless of their clustercentric distance. The final mass-limited ICBS sample with $M_* \geq 10^{10.5}\,\mathrm{M}_\odot$ consists of 371 galaxies. Considering also the completeness weights, the number of galaxies is 754. The field galaxy sample consists of 275 galaxies, 658 once weighted.

2.4 EDisCS

For intermediate-redshift clusters, we also use galaxies that belong to the EDisCS, which is a multiwavelength photometric and spectroscopic survey of galaxies in 20 fields containing galaxy clusters at $0.4 < z < 1$ (White et al. 2005). EDisCS clusters were drawn from the Las Campanas Distant Cluster Survey (LCDCS) catalogue (Gonzalez et al. 2001). They were selected as surface brightness peaks in smoothed images taken with a very wide optical filter (∼4500–7500 Å), and have high-quality multiband optical and near-infrared photometry (White et al. 2005) and spectroscopy (Halliday et al. 2004; Milvang-Jensen et al. 2008).

Photometric redshifts were computed for each object in the EDisCS fields using two independent codes, a modified version of the publicly available HYPERZ code (Bolzonella, Miralles & Pelló 2000) and the code of Rudnick et al. (2001) with the modifications presented in Rudnick et al. (2003, 2009). The accuracy of both methods is $\sigma(\delta z) \sim 0.05$–$0.06$, where $\delta z = [(z_{\mathrm{spec}} - z_{\mathrm{phot}})/(1 + z_{\mathrm{spec}})]$. Photo-$z$ membership (see also De Lucia et al. 2004, 2007 for details) was established using a modified version of the technique first developed in Brunner & Lubin (2000), in which the probability of a galaxy to be at redshift z $[P(z)]$ is integrated in a slice of $\Delta z = \pm 0.1$ around the cluster redshift to give P_{clust} for the two codes. A galaxy was rejected from the membership list if P_{clust} was smaller than a certain probability P_{thresh} for either code. The P_{thresh} value for each cluster was calibrated from our spectroscopic redshifts and was chosen to maximize the efficiency with which we can reject spectroscopic non-members while retaining at least ∼90 per cent of the confirmed cluster members, independent of their rest-frame $(B-V)$ colour or observed $(V-I)$ colour.

In Vulcani et al. (2010), we estimated galaxy stellar masses using photo-z fitting total absolute magnitudes (Pelló et al. 2009) and, using, as for other surveys, the relation between mass-to-light ratio M/L_B and rest-frame $(B-V)$ colour for solar metallicity from Bell & de Jong (2001). The photometric magnitude limit ($I = 24$) corresponds to a mass limit of $\log M_*/\mathrm{M}_\odot = 10.2$ (Vulcani et al. 2010).

The projected local galaxy density is derived from the circular area A that in projection on the sky encloses the N closest galaxies brighter than an absolute V magnitude $M_V \leq -20$. We use $N = 10$, as in WINGS and in most previous studies in clusters. Since for about only 7 per cent of the galaxies in our sample the circular region containing the 10 nearest neighbours extends off the chip and local densities only of these sources suffer from edge effects, we do not use any interpolation technique, but simply excluded those galaxies from our analysis.

As largely discussed in Poggianti et al. (2008), we apply three different methods to identify the 10 cluster members that are closest to each galaxy. These yield three different estimates of the projected local density, which we compare in order to assess the robustness of our results. Briefly, in the first method, the density is calculated using all galaxies in our photometric catalogues and is then corrected using a statistical background subtraction. In the other two methods we include only those galaxies that are considered cluster members according to photometric redshift estimates. We use two different criteria to identify photo-z neighbours. In the first case, a galaxy is accepted as neighbour if it is a cluster member according to the photo-z membership criteria described above. In the other method, a galaxy is retained as neighbour if the best photometric estimate of its redshift from the HYPERZ code is within 0.1 in z from the cluster redshift.

Since all the methods give results that are in good agreement, in the following we show only the analysis of the second method, defining galaxy neighbours according to photo-z membership using the integrated probability.

In this work, we use photo-z members of all the EDisCS clusters (see Table 2 for the list of clusters) and we consider a mass-limited sample of galaxies with $\log M_*/\mathrm{M}_\odot \geq 10.2$. We take into account all cluster galaxies, regardless of their clustercentric distance, but we exclude the BCGs, as we do in WINGS, since their presence could alter the mass distributions. The final EDisCS sample consists of 1560 galaxies.

3 RESULTS

Above the mass completeness limit, we subdivide the galaxies of each sample into four bins of local density, so that in the two central bins galaxies are twice as numerous as galaxies in the outer bins. Since the choice of the number of bins and of their limits is arbitrary, we also tried subdividing galaxies into two, three, six, eight bins and checked that the final conclusions are stable and independent from the choice made.

Table 2. List of EDisCS clusters analysed in this paper, with cluster name, redshift z and velocity dispersion σ (from Halliday et al. 2004; Milvang-Jensen et al. 2008).

Cluster name	z	σ (km s^{-1})
cl 1018.8-1211	0.47	486^{+59}_{-63}
cl 1040.7-1155	0.70	418^{+55}_{-46}
cl 1054.4-1146	0.70	589^{+78}_{-70}
cl 1054.7-1245	0.75	504^{+113}_{-65}
cl 1059.2-1253	0.46	510^{+52}_{-56}
cl 1138.2-1133	0.48	732^{+72}_{-76}
cl 1202.7-1224	0.42	518^{+92}_{-104}
cl 1216.8-1201	0.79	1018^{+73}_{-77}
cl 1227.9-1138	0.64	574^{+72}_{-75}
cl 1232.5-1250	0.54	1080^{+119}_{-89}
cl 1301.7-1139	0.48	687^{+81}_{-86}
cl 1353.0-1137	0.59	666^{+136}_{-139}
cl 1354.2-1230	0.76	648^{+105}_{-110}
cl 1411.1-1148	0.52	710^{+125}_{-133}

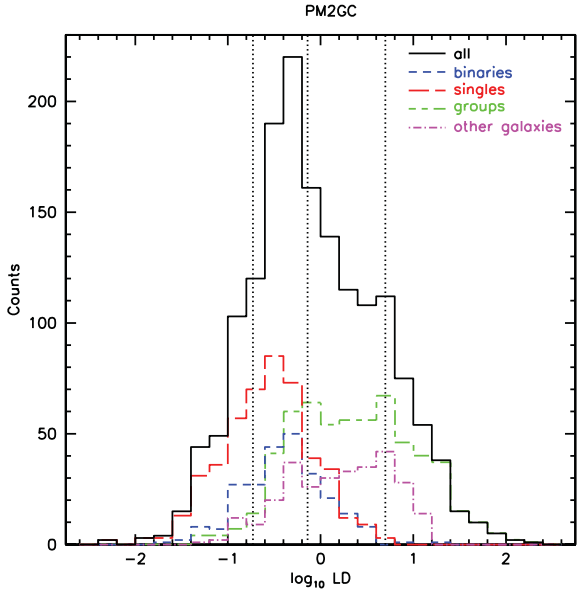

Figure 1. Local density distribution of PM2GC galaxies at $z = 0.03$–0.11 with $\log M_*/\mathrm{M}_\odot \geq 10.25$ for the whole field and the different global environments. The vertical dotted lines represent the limits of our four density bins.

In each bin of local density, we build histograms to define the mass distribution. In each mass bin, we sum all galaxies to obtain the total number of galaxies, then we divide this number by the width of the bin, to have the number of galaxies per unit mass. The width of each mass bin is 0.2 dex. For building histograms of the WINGS and ICBS samples, each galaxy is weighted by its incompleteness correction. Error bars on the x-axis represent the width of the bin, and error bars on the y-axis are computed using Poissonian errors (Gehrels 1986).

In each of the following figures representing the mass functions, we have normalized the curves so that the number of objects in the intermediate-mass bins ($10.8 \leq \log M_*/\mathrm{M}_\odot \leq 11.2$) is the same in all the mass functions plotted. In this way, the differences at lower and higher masses are easily visible at a glance.[3] We focus our attention mainly on the shape of the mass distribution.

With these aims, we use the Kolmogorov–Smirnov (KS) test and also visually analyse the plots. The KS test tells us whether we can disprove the null hypothesis that two data sets are drawn from the same population distribution function. The standard KS test, in building the cumulative distribution, assigns to each object a weight equal to 1. Instead, our WINGS and ICBS data are characterized by spectroscopic completeness weights. So, when we study WINGS and ICBS galaxies, we modified the test, to make the relative importance of each galaxy in the cumulative distribution depend on its weight, and not being fixed to 1. A 'positive' (statistically significant) KS result robustly highlights the differences between two distributions, but a negative KS result does not mean that the distributions are similar. In particular, as we will see, when adopting low galaxy mass limits, the KS test is not sensitive to mass segregation at the high-mass end simply because there are relatively few galaxies at high mass and they are not able to sufficiently influence the cumulative distribution upon which the KS test is based. Therefore, it is necessary to inspect the mass distributions, and their upper mass, beyond the KS test.

In the following, we present the results of our analysis for each of our four galaxy samples. We start analysing the relation between mass distribution and environment in the local Universe in the general field, in order to consider a range of local density as large as possible. Then, we focus our attention only on clusters, to see if they behave as galaxies in the general field. Subsequently, we move on to higher redshift, where we again analyse both field and cluster galaxies.

We stress that we are not able to cross-compare our samples, either at a given epoch or as a function of epoch. Since densities are defined in different ways for each of the four samples (see Sections 2.1–2.4), the results of the inter-sample analysis would be difficult to interpret.

3.1 General field at low-z

We use the PM2GC data set to describe galaxies in the general field in the local Universe. Fig. 1 shows the distribution of the local density in this sample and the limits adopted to subdivide galaxies into four bins. We can immediately see that the range of local densities spanned is very wide, covering almost 4 dex. Even if at first we will consider the general field altogether, it is useful to inspect the local density distributions of group, binary and single galaxies separately, as shown in Fig. 1.[4] Single galaxies are preferentially located in the lowest density bins, groups in the highest and binaries in the intermediate range. In particular, in the lowest density bin, the contribution of groups is almost negligible, while in the highest bin, single and binary galaxies are almost absent. Each environment, however, spans at least three of our density bins.

[3] We remind the reader that the normalization adopted in displaying the mass functions does not influence the KS test and hence our results.

[4] For the sake of completeness, 'other galaxies' are also plotted; they include all galaxies that belong to groups but are outside each group radial limit or the redshift range for groups.

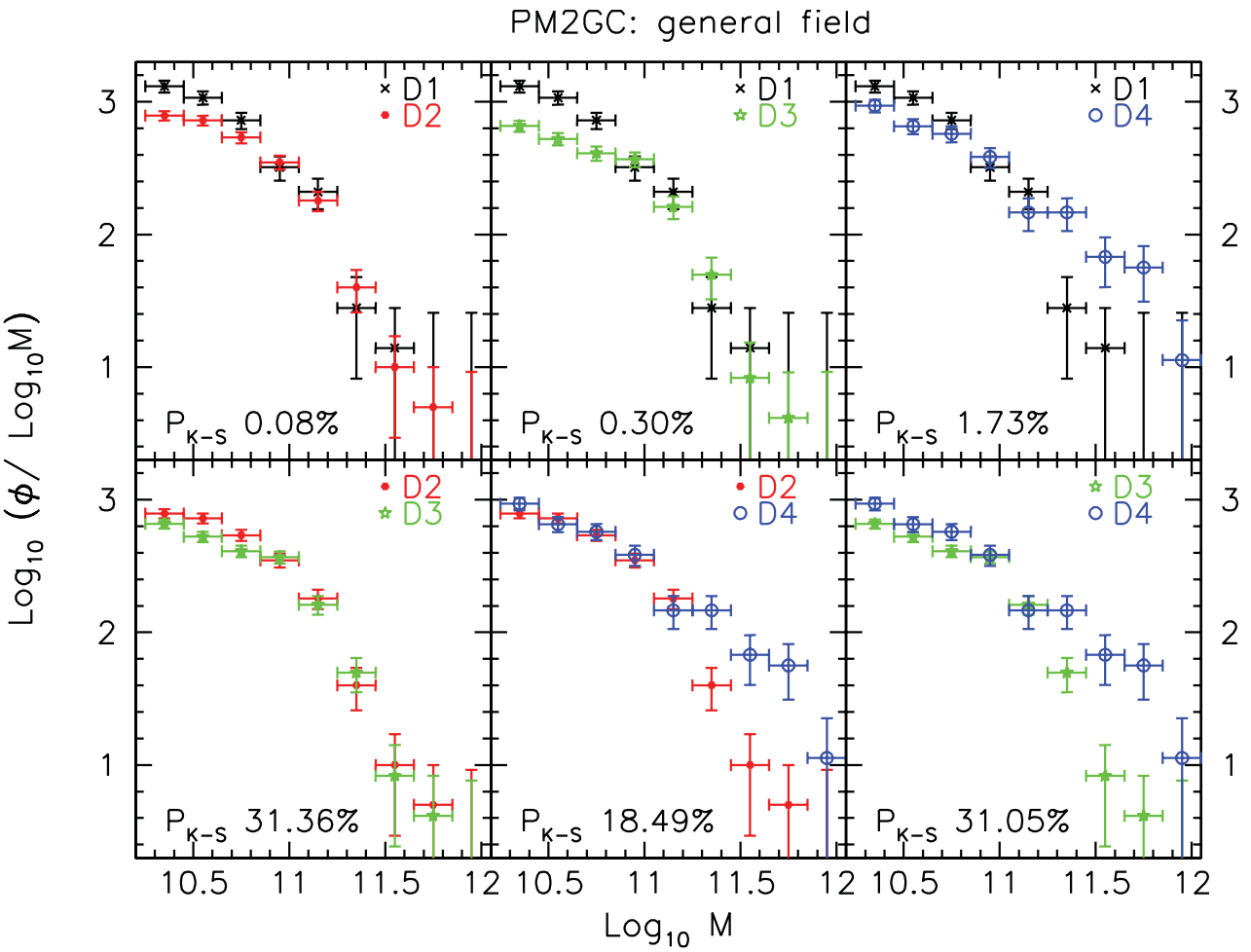

Figure 2. Low-z field (PM2GC): galaxy stellar mass functions in four different bins of local density, compared two by two. The curves are normalized so that the number of galaxies at intermediate masses ($10.8 \leq \log M_*/\mathrm{M}_\odot \leq 11.2$) is the same. Black crosses: D1 (lowest density bin); red filled points: D2; green filled stars: D3; blue empty points: D4 (highest density bin). Results of the KS test are also indicated. The mass function depends on local density: lower density bins have proportionally a larger population of low-mass galaxies than higher density regions.

In Fig. 2 we show the mass functions of galaxies in different density bins, compared two by two. We find that the mass function depends on local density: lower density bins have proportionally a larger population of low-mass galaxies than higher density regions.

The KS test can reject the null hypothesis that the distributions are drawn from the same parent distribution when we compare D1 with all the other bins, while it is inconclusive in all other cases. However, looking at the figure, it clearly emerges that the slope of the D4 mass function at masses above $M_*/\mathrm{M}_\odot \sim 10^{11}$ is much shallower than the slope in any other density bin, and that with the normalization adopted it is equivalent to say that in the highest density bin D4 there is an 'excess' of high-mass galaxies, compared to the other bins. To substantiate this on statistical grounds, since galaxies in the lowest mass bins are very numerous and they probably strongly influence the KS test results, we try pushing up the mass limit so as to exclude those galaxies from the analysis. Redefining the mass limit entails a slight change in the limits of the local density bins, so we compute them again.[5] For $\log M_*/\mathrm{M}_\odot \geq 10.5$, the differences in the mass function between D4 and the other density bins become statistically significant.

In general, even for a very high-mass threshold ($\log M_*/\mathrm{M}_\odot \geq 10.8$), the differences in the mass functions of galaxies in different density bins remain statistically significant, showing that local density matters for any mass limit adopted.

As seen in Fig. 1, galaxies in groups, binary systems and single galaxies cover different ranges of local densities; therefore, we now wish to test whether our local density results are driven by galaxies in specific global environments (for example, only in massive groups). Therefore, we tried excluding single galaxies or galaxies located in massive groups ($\sigma_{\mathrm{group}} > 400\,\mathrm{km\,s^{-1}}$ and $\sigma_{\mathrm{group}} > 500\,\mathrm{km\,s^{-1}}$) (plots not shown). In all these cases, we always find a similar dependence of the mass functions on the local density as we see in the general field. Therefore, the variations of the mass distributions with local density are not driven by a different dependence in a specific global environment.

[5] From now on, when we change the mass limit, we always compute again the limits of the density bins: each time, above the adopted mass limit we subdivide galaxies so that in the two central bins galaxies are twice as numerous as galaxies in the outer bins.

3.2 Clusters at low-z

We use the WINGS data set to study galaxies in clusters in the local Universe. Fig. 3 shows the distribution of local densities in

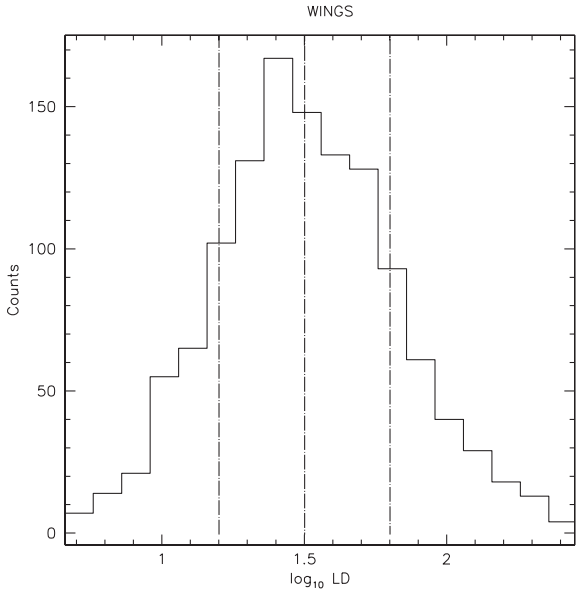

Figure 3. Local density distribution of WINGS galaxies at $z = 0.04$–0.07 with $\log M_*/\mathrm{M}_\odot \geq 9.8$. The vertical dotted lines represent the limits of our four density bins.

this sample and the four density bins. In clusters, galaxies cover a range of local density of about 1.8 dex.

In Fig. 4 we show the mass function of galaxies in the different bins of local density, compared two by two.[6] Also in the case of clusters, there is a dependence of the mass function on the local density. In general (except when we compare D3 and D4 whose shapes are very similar), lower density bins have proportionally a greater number of lower mass galaxies. The KS test can reject the hypothesis of a common parent distribution with a high level of significance in most of the cases.

We note that, unlike the mass function in the general field at the same redshift, in clusters the mass functions in the highest density bin (D4, and perhaps D3) flatten out at low galaxy masses, below $\log M_*/\mathrm{M}_\odot \sim 10.5$. This is suggestive of a sort of 'deficit' of low-mass galaxies with respect to intermediate masses compared to lower density regions.

As before, the KS test is particularly sensitive to the large number of low-mass galaxies, so we push up the mass limit in order to detect possible differences in the slope of the mass functions at high mass. After redefining the density bins, we find that local density effects in low-z clusters are not visible at intermediate–high galaxy masses, as the KS test finds differences between the mass function of galaxies in different density regions only for a mass limit of $\log M_*/\mathrm{M}_\odot \leq 10.1$. This limit is even lower than the mass completeness limit of the PM2GC survey. In contrast, as we have seen in Section 3.1 for the PM2GC, the local density effects in the general field on the shape of the mass function do not disappear at any mass.

3.3 Field at intermediate-z

We use the field sample of the ICBS data set to characterize galaxies in the field at intermediate redshifts. Fig. 5 shows the distribution of the local density in this sample and the four density bins. In the histogram, very isolated galaxies without an estimate of local density (see Section 2.3) are assigned $\log(LD) = -1.5$. We can immediately see that, excluding very isolated galaxies, for which we do not have a real estimate of local density, the range of local densities spanned is very wide, covering almost 4 dex. This range is also very similar to that we found for the PM2GC, indicating that actually the (general) field is a very heterogeneous environment, with very sparse regions but also with highly populated ones.

In Fig. 6 we present the mass functions of galaxies in different density bins, compared two by two. Again, the mass function depends on local density in the sense that lower density regions have proportionally a larger population of low-mass galaxies than higher density regions.

Despite the quite small number statistic, the KS test can always reject the null hypothesis that the distributions are drawn from the same parent distribution except when we compare D1 and D2. Moreover, looking at the figure, as in the PM2GC, we find that the slope of the D4 (and maybe D3) mass function at masses above $M_*/\mathrm{M}_\odot \sim 10^{11.2}$ is shallower than the slope in the other density bins, indicating a possible 'excess' of high-mass galaxies in that bin, compared to the other bins.

In this case, we decide not to further push up the mass limit, both because it is already fairly high and because the statistical uncertainty would be too large.

3.4 Clusters at intermediate-z

We use the EDisCS data set to describe galaxies in distant clusters.

Fig. 7 shows the distribution of the local density in this sample and the limits of the four density bins. In clusters at high-z, galaxies can assume local density values in a range of almost 2.3 dex.

In Fig. 8 we show the mass functions of galaxies in the different bins, compared two by two. As for WINGS, we find that there is a clear dependence of the mass function on the local density, in the sense that low-density regions have proportionally more low-mass galaxies. The KS test is able to refuse the null hypothesis of similarity of the populations in the majority of cases.

Again, as for WINGS, also in distant clusters the mass functions in the highest density bin (D4, and perhaps D3) flatten out at low galaxy masses.

Adopting a higher mass limit, we find that for $\log M_*/\mathrm{M}_\odot \geq 10.4$, the KS results are inconclusive, suggesting again that in clusters the effects of the local density on the high-mass-end shape of the mass function are not visible.

Using the ICBS cluster sample (plots not shown), above the mass limit of $\log M_*/\mathrm{M}_\odot > 10.5$, we find that the local density range spanned is $\sim$2.5 dex, very similar to that of EDisCS. Moreover, in agreement with the EDisCS findings, we find no dependence at such high masses.

4 GENERAL TRENDS

Our results show that at both redshifts and in all environments, there is a dependence of the mass function on the local density. Even if we cannot perform any inter-sample comparison, since densities have been computed using different criteria, in the following we can qualitatively compare our results coming from the different surveys, to detect if a common trend does exist.

In general, the lower the density, the higher is (proportionally) the number of low-mass galaxies, indicating that low-mass galaxies are more common in the 'sparsest' regions.

[6] We remind the reader that the WINGS sample is not spectroscopically complete, so in all the following analyses, we always take into account WINGS' weights.

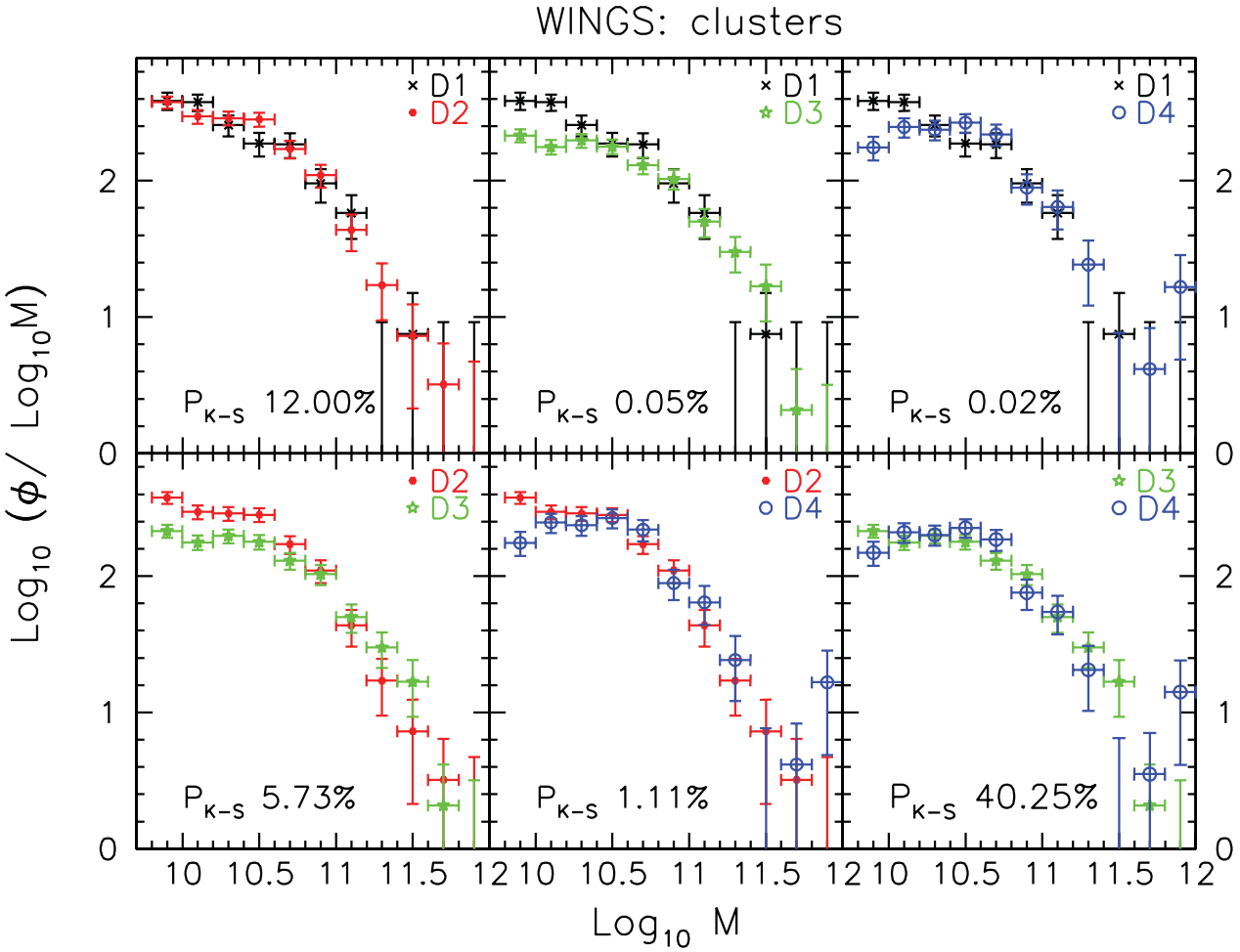

Figure 4. Low-z clusters (WINGS) galaxy stellar mass functions in four different bins of local density, compared two by two. The curves are normalized so that the number of galaxies at intermediate masses ($10.8 \leq \log M_*/\mathrm{M}_\odot \leq 11.2$) is the same. Black crosses: D1; red filled points: D2; green filled stars: D3; blue empty points: D4. Results of the KS test are also indicated. As for the general field, the mass function depends on local density: in general, lower density bins have proportionally a larger population of low-mass galaxies than higher density regions.

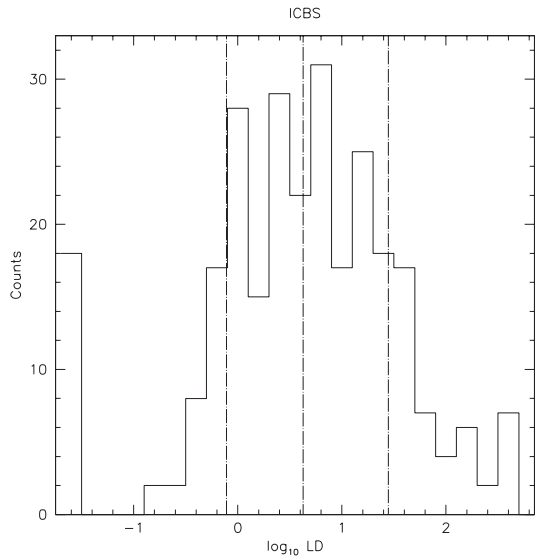

Figure 5. Local density distribution of ICBS galaxies at $z = 0.25$–0.45 with $\log M_*/\mathrm{M}_\odot \geq 10.5$ for the field. Very isolated galaxies without an estimate of local density (see Section 2.3) are assigned $\log(LD) = -1.5$. The vertical dotted lines represent the limits of our four density bins.

Fig. 9 shows the cumulative distributions of PM2GC, WINGS, ICBS-field and EDisCS and summarizes the main result: in higher density regions, galaxies are proportionately more massive, indicating that the mass function shape changes with local density [the colour progression black (D1), red (D2), green (D3), blue (D4) is always the same].

Galaxies in D1, D2, D3 and D4 reach a different upper mass. In particular, very massive galaxies (having excluded the cluster BCGs) seem to be located only in the highest density bin, while they are absent at lower densities. For example, in the PM2GC, the most massive galaxy in D1 has $\log M_*/\mathrm{M}_\odot = 11.5$, the most massive galaxy in D2 and D3 has $\log M_*/\mathrm{M}_\odot = 11.7$, while the most massive galaxy in D4 has $\log M_*/\mathrm{M}_\odot = 11.9$. In WINGS, neither D1, D2 nor D3 hosts galaxies more massive than $\log M_*/\mathrm{M}_\odot = 11.6$, while D4 is also populated by galaxies with $11.6 \leq \log M_*/\mathrm{M}_\odot \leq 12$. This supports the mass segregation scenario for the very most massive galaxies.

Not only the maximum mass but also the average mass depends on density, as shown in Fig. 10 separately for each sample. In the figure, the logarithmic mean mass computed in each density bin is plotted versus the logarithmic mean density. The average mass allows us to have an immediate comparison among the different characteristic masses at the different local densities, and to see how the mean mass

© 2011 The Authors, MNRAS **420,** 1481–1494
Monthly Notices of the Royal Astronomical Society © 2011 RAS

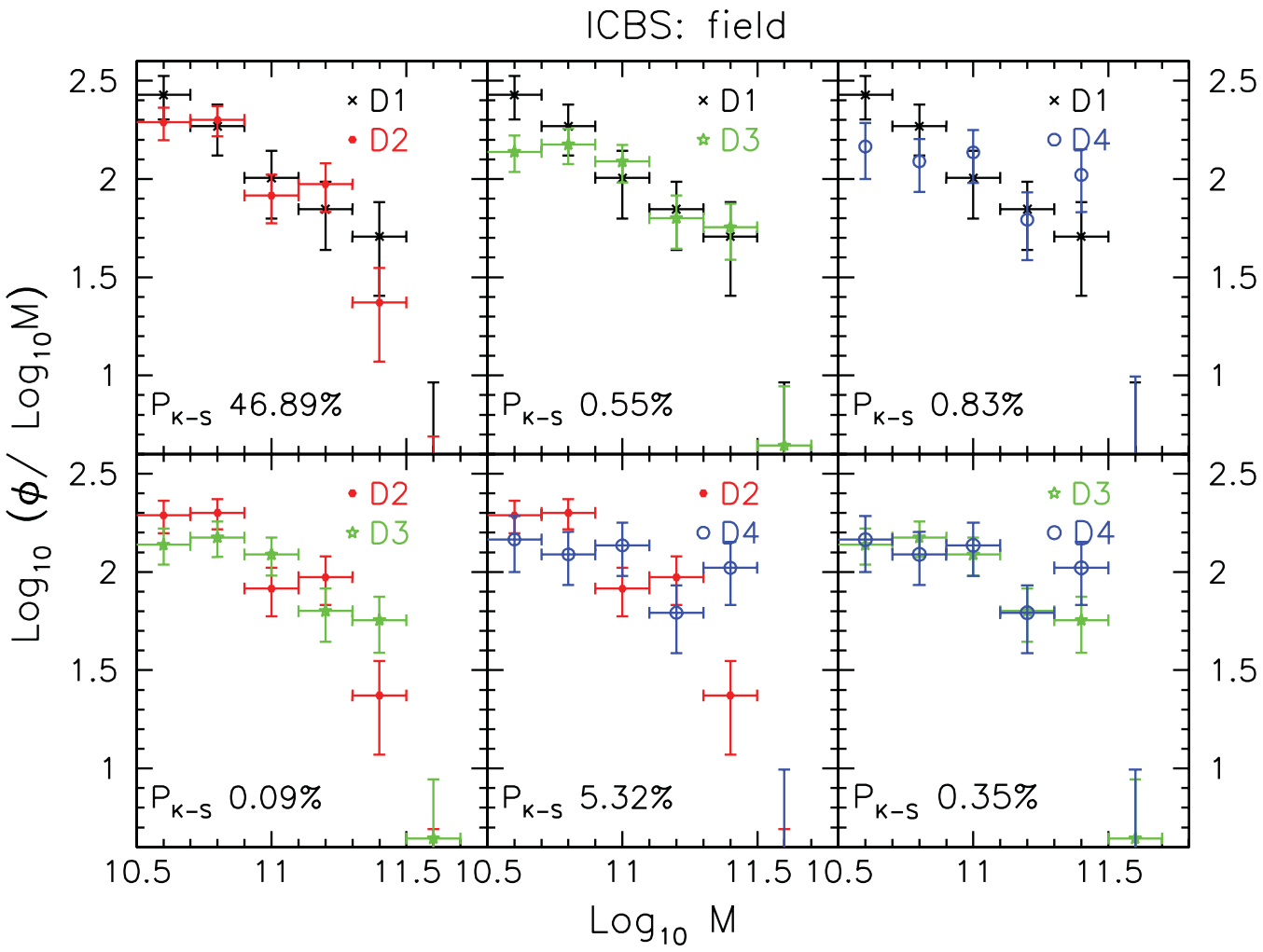

Figure 6. Intermediate-z field (ICBS): galaxy stellar mass functions in four different bins of local density, compared two by two. The curves are normalized so that the number of galaxies at intermediate masses ($10.8 \leq \log M_*/\mathrm{M}_\odot \leq 11.2$) is the same. Black crosses: D1 (lowest density bin); red filled points: D2; green filled stars: D3; blue empty points: D4 (highest density bin). Results of the KS test are also indicated. The mass function depends on local density: lower density regions have proportionally a larger population of low-mass galaxies than higher density regions.

changes as a function of the LD in each sample. In all samples, only galaxies above the mass limit of the sample are considered; hence, mean masses cannot be directly compared in the different samples. We find a common trend in all samples: as might be expected based on the results shown before, the average mass is higher in higher density bins. In the local Universe, both in the field and in clusters, the $\Delta(\log\langle M\rangle)$ is about 0.2 dex, at intermediate redshift in the field it is slightly higher [$\Delta(\log\langle M\rangle) \sim 0.25$ dex] while in distant clusters the difference between the mean mass in the lowest and the highest density bins is greater [$\Delta(\log\langle M\rangle) \sim 0.5$ dex]: on average, galaxies in D4 are much more massive than in other bins.

Moreover, Fig. 9 shows that galaxies more massive than $\log M_*/\mathrm{M}_\odot \sim 11$ [which represent 22, 22, 37 and 36 per cent of all galaxies more massive than $\log M_*/\mathrm{M}_\odot = 10.5$ in PM2GC, WINGS, ICBS and EDisCS, respectively[7]] are not confined to the highest density regions: about 20 per cent of them are in D4, and about 70 per cent in D2+D3, in all the samples.

So far, in the literature, several works analysed galaxies located in regions characterized by different densities (all of them for galaxies in the general field). For the local Universe, Kauffmann et al. (2004) and Baldry et al. (2006) focused their attention on a wide range of local densities, while at higher redshift Bundy et al. (2006) and Bolzonella et al. (2010) focused mainly on the extreme environments, usually comparing D1 and D4, neglecting intermediate regions. Our results are in agreement with their results. In addition, in most cases we also find differences in the mass function of galaxies in contiguous density bins.

5 GLOBAL AND LOCAL ENVIRONMENTS

We have seen that (general) field and clusters seem to qualitatively behave in a quite different way. In the local general field, the local density can influence the stellar mass function at any mass: comparing the mass function in different density bins, differences in the mass function slope are visible both in the low-mass regime

[7] The fact that at low and intermediate redshifts we find the same fraction of massive galaxies indicates that the evolution of the fraction is independent of environment.

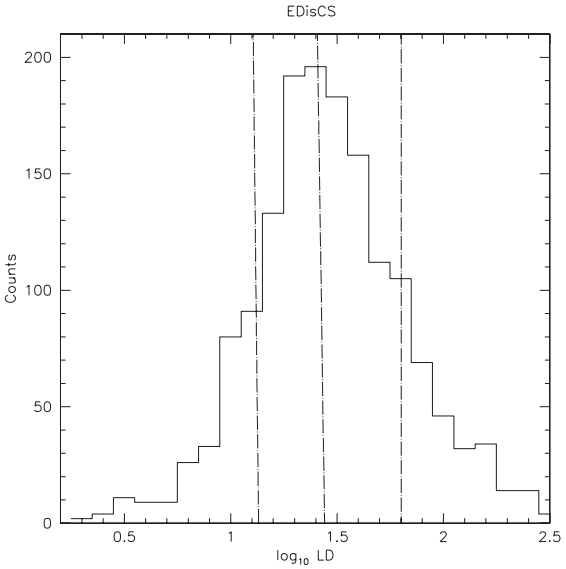

Figure 7. Local density distribution of EDisCS galaxies with $z = 0.4$–0.8 with $\log M_*/\mathrm{M}_\odot \geq 10.2$. The vertical dotted lines represent the limits of our four density bins.

and at the high-mass end. In the higher redshift field, local density influences the mass distribution at high masses, but the rather high-mass limit does not allow us to inspect lower masses. On the other hand, in clusters, the biggest differences are always confined at low masses, while the shape of the mass function of intermediate-massive galaxies seems not to be strongly affected by the local density.

In principle, the different behaviour observed in the field and clusters could be due to two different reasons: the smallest local density range sampled in clusters or a residual dependence on the global environment.

In the local Universe, since the density range investigated with WINGS is relatively small [$\Delta(\log\langle\Sigma\rangle) = 1.8$ dex], it is possible that this range of densities corresponds to only the highest density regions in the PM2GC, which spans $\Delta(\log\langle\Sigma\rangle) = 4$ dex. Unfortunately, there is no way to directly compare the local densities in the two samples to surely assess how the density ranges overlap. In any case, since the PM2GC also contains high-velocity dispersion structures, we have analysed their density distribution separately. First of all, we have checked that the PM2GC 'clusters' (groups with $\sigma_{\mathrm{group}} > 500\,\mathrm{km\,s^{-1}}$) cover a range of local density very similar to that spanned by *all* groups; hence, their galaxies are also located in low-density regions (D1 and D2). Secondly, we have

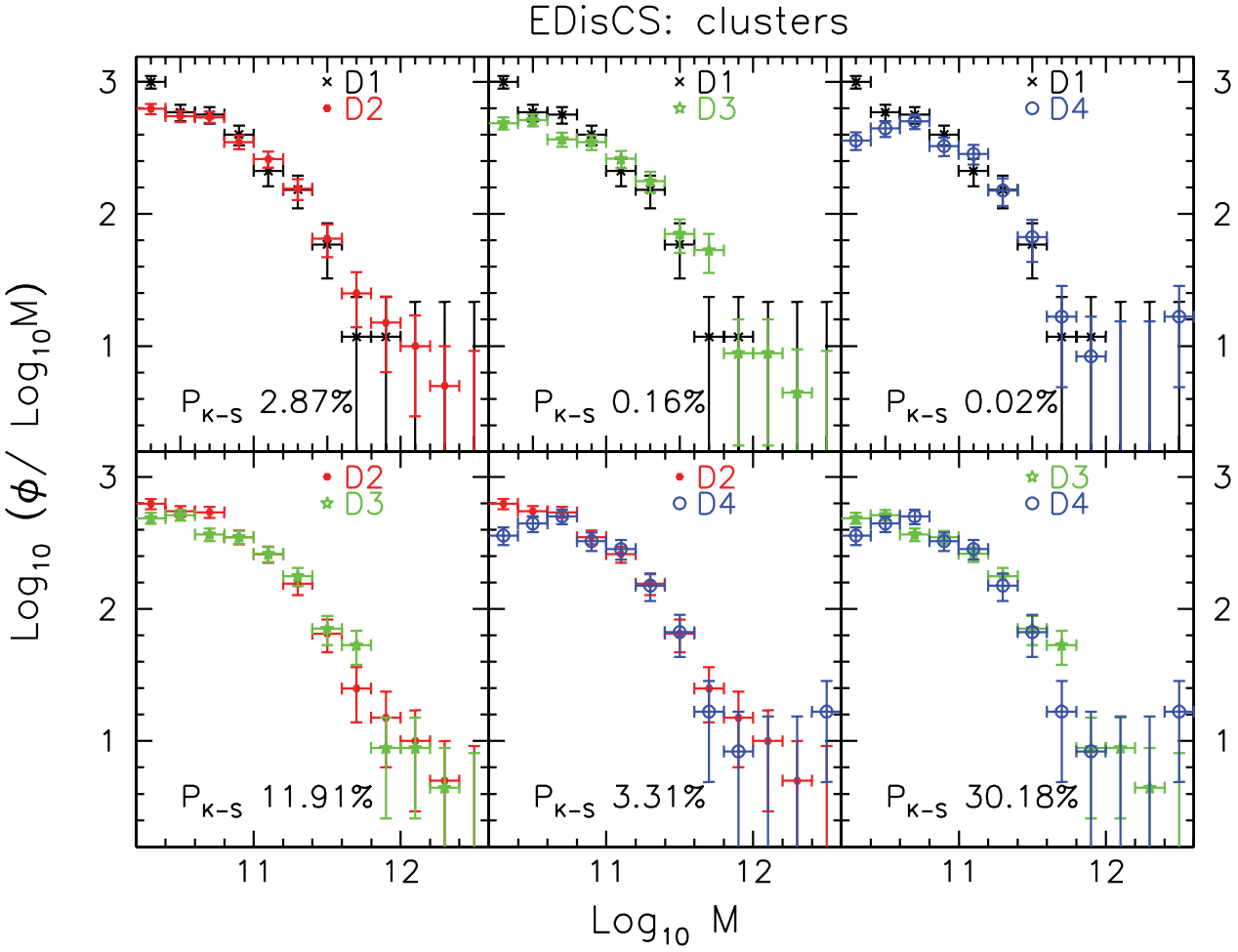

Figure 8. Intermediate-z clusters (EDisCS) galaxy stellar mass functions in four different bins of local density, compared two by two. The curves are normalized so that the number of galaxies at intermediate masses ($10.8 \leq \log M_*/\mathrm{M}_\odot \leq 11.2$) is the same. Black crosses: D1; red filled points: D2; green filled stars: D3; blue empty points: D4. Results of the KS test are also indicated. As for clusters in the local Universe, there is a clear dependence of the mass function on the local density: low-density regions have proportionally more low-mass galaxies.

© 2011 The Authors, MNRAS **420,** 1481–1494
Monthly Notices of the Royal Astronomical Society © 2011 RAS

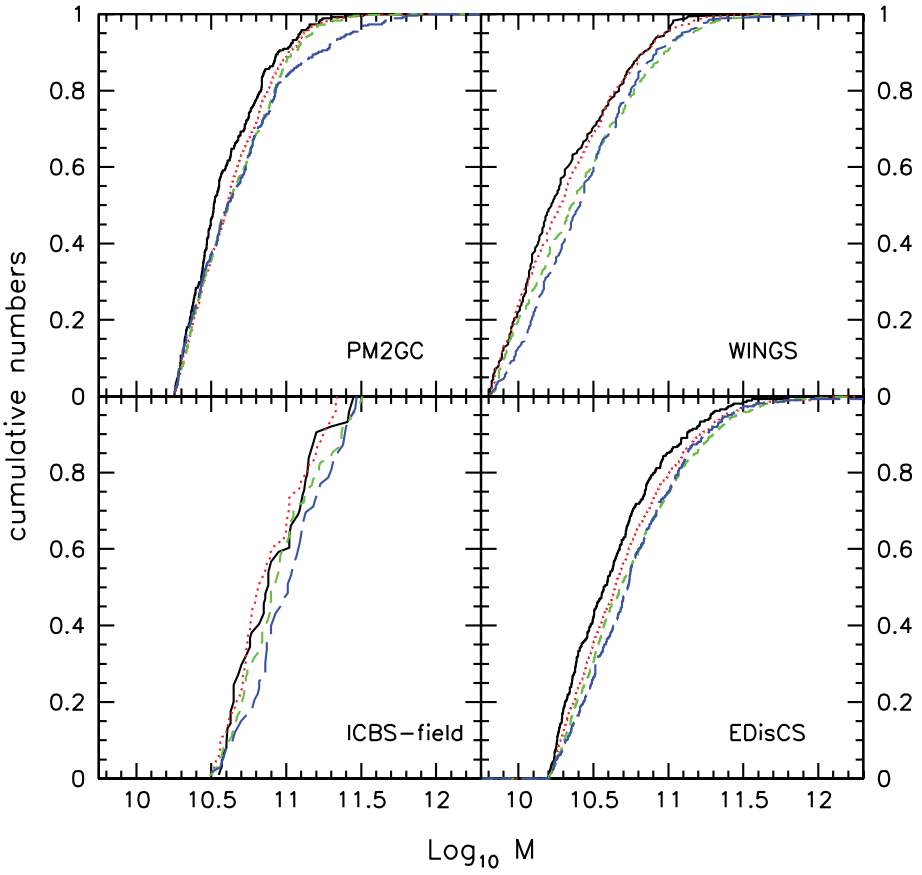

Figure 9. Cumulative distributions of PM2GC (top left panel), WINGS (top right panel), ICBS (bottom right panel) and EDisCS (bottom left panel). In all panels, black solid lines represent the lowest density bin D1, red dotted lines D2, green dashed lines D3 and blue long dashed lines D4. In all samples, the lower the density, the higher is proportionally the number of low-mass galaxies. Moreover, the highest masses reached at different densities are also different.

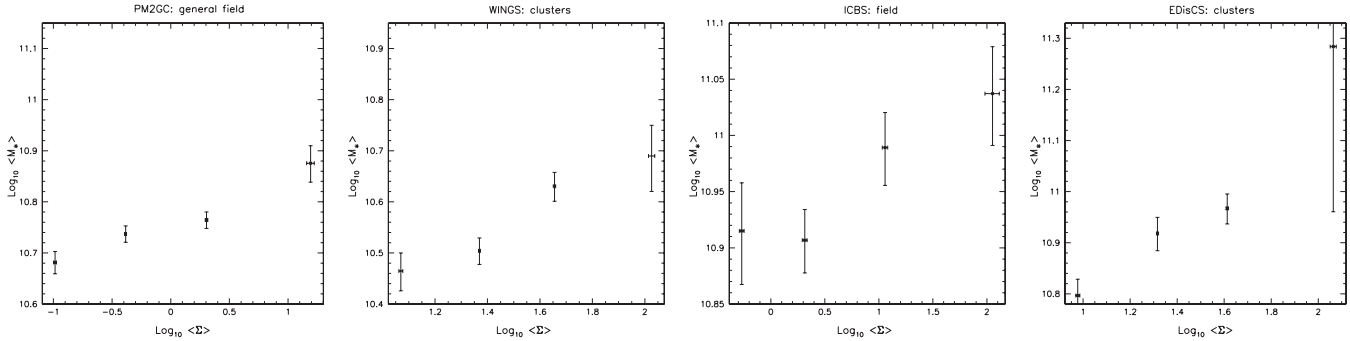

Figure 10. Mass–local density relation for the PM2GC (left-hand panel), WINGS (central left panel), ICBS (central right panel) and EDisCS (right-hand panel) surveys. For each sample, above its proper mass completeness limit, the mean mass has been computed separately in the four density bins. Errors are defined as $\mathrm{rms}/\sqrt{N}$, where N is the number of galaxies in each density bin. For WINGS and ICBS, weighted means are computed. In all samples, the average mass depends on local density: the average mass is higher in higher density bins.

checked the host structure of galaxies in the highest density bin D4 and found that actually only 43 per cent of galaxies in D4 belong to a structure with a velocity dispersion of $\sigma > 400\,\mathrm{km\,s^{-1}}$ and 30 per cent belong to a structure with $\sigma > 500\,\mathrm{km\,s^{-1}}$. Therefore, D4 is also populated by galaxies in smaller systems not comparable to the cluster environment. On the other hand, 38.2 per cent (44.3 per cent) of galaxies in PM2GC structures with $\sigma > 400\,\mathrm{km\,s^{-1}}$ (500) are located in D4, 34.5 per cent (35.0 per cent) in D3, 19.9 per cent (18.4 per cent) in D2 and 7.4 per cent (2.3 per cent) in D1, indicating that most of PM2GC cluster galaxies are hosted in rather high-density regions.

At higher redshift, we have at our disposal both the field and cluster galaxies from the ICBS, besides EDIsCS clusters. As in the local Universe, the local density ranges spanned are different in clusters and field: $\Delta(\log\langle\Sigma\rangle) = 2.5$ dex versus $\Delta(\log\langle\Sigma\rangle) = 4$ dex.

As a consequence, the different local density distributions covered by the different samples could be responsible for the different trends we have detected in clusters and (general) field.

As we have seen in Section 3.1 for the most massive groups in the PM2GC, in the field at low-z the local density trends of the mass functions do not seem to be due to the global environment. To assess in detail the role of the global environment, in separate papers we have analysed how the galaxy stellar mass function depends on it. Using the PM2GC and WINGS data, in Calvi et al. (in preparation), we find that the shape of the mass distribution does not depend on whether galaxies belong to a galaxy system (group or cluster) or not. Indeed, we are not able to detect any substantial difference in the shape of the cluster, group and field mass functions. In Vulcani et al. (2011b), we have carried out a similar analysis on galaxies located at higher redshift ($z \sim 0.3$–0.8), exploiting the capabilities of the ICBS and EDisCS. Again, our findings suggest a universality of the mass distribution in different global environments (clusters, groups and field), at least for galaxies above the mass limit of our samples ($\log M_*/\mathrm{M}_\odot \geq 10.2$–$10.5$). Summarizing, in those works we do not detect a dependence of the mass distribution on the global environment. Hence, in our samples, above the same mass we use here (that corresponds to the two mass limits), we detect differences among mass distributions of galaxies located at different local densities but not in different global environments.

As a consequence, the evidence that the mass function does depend on local density raises an interesting question. Why does local density play a more active role than global environment in shaping the mass function, at both redshifts?

Recently, other evidence has been accumulated that the local environment is more important than the global environment in also shaping several of the main galaxy properties, not just the galaxy mass. The results for two of these properties are most striking and concern the red galaxy population and the morphological types of galaxies.

In WINGS clusters, none of the characteristics of the colour–magnitude red sequence (slope, scatter, luminous-to-faint ratio, blue fraction and morphological mix on the red sequence) depends on global cluster properties connected with cluster mass, such as cluster velocity dispersion and X-ray luminosity. In contrast, *all* of these characteristics vary systematically with the local galaxy density (Valentinuzzi et al. 2011).

Also in WINGS, we have shown that the fractions of spiral, S0 and elliptical galaxies do not vary systematically with cluster velocity dispersion and X-ray luminosity (Poggianti et al. 2009), while a strong morphology–density relation is present in WINGS as in any other sample (Fasano et al., in preparation).

In addition, Balogh et al. (2004), analysing the colour distribution of bright ($M_r \leq 18$) galaxies in the local Universe ($z < 0.08$), found that the red fraction of galaxies is a strong function of local density, increasing from ∼10–30 per cent of the population in the lowest density environments to ∼70 per cent at the highest densities, while within the virialized regions of clusters it shows no significant dependence on cluster velocity dispersion.

Also, Martínez, Coenda & Muriel (2008) found that bright galaxy properties do not clearly depend on cluster mass for clusters more massive than $M \sim 10^{14}\,\mathrm{M}_\odot$, while they correlate with cluster-centric distance.

Our results on global and local environments now allow and require a comparison with theoretical expectations, to understand whether simulations predict a mass segregation with environment, both considering the initial and evolved halo mass and the local density, and how they predict the evolution with redshift as a function of the environment.

6 CONCLUSIONS

In this paper, we have tried to quantify the importance of the local density in shaping the stellar galaxy mass function of galaxies located in different environments both at low and intermediate redshifts taking directly into account also the cluster environment.

Our main conclusion is that at all redshifts and in all environments, local density plays a significant role in driving the mass distribution.

In the general field at low-z, local density influences the stellar mass distribution both at low and high masses. In the field at high-z, the dependence exists at high masses, while our mass limit does not allow us to inspect low masses. On the other hand, in clusters, the biggest differences are always confined at low masses. If we perform a higher mass cut ($\log M_*/\mathrm{M}_\odot > 10.1$ for WINGS and $\log M_*/\mathrm{M}_\odot > 10.4$ in EDisCS), every difference in slope disappears.

We have found that not only the shape of the mass function depends on local density, but also the highest mass reached in each density bin: very massive galaxies (having excluded the cluster BCGs) seem to be located only in the highest density bin while they are absent at lower densities (the so-called mass segregation).

Comparing our results with those of Calvi et al. (in preparation) and Vulcani et al. (2011b) for the global environment, we conclude that local environment plays a much more visible role than global environment in shaping the stellar galaxy mass distribution.

ACKNOWLEDGMENTS

We thank the referee for useful comments. We would like to thank the whole WINGS team for stimulating discussions. We would also like to thank Alfonso Aragón-Salamanca and Gabriella De Lucia, whose suggestions helped us to improve the paper. BV and BMP acknowledge financial support from ASI contract I/016/07/0 and ASI-INAF I/009/10/0. BV also acknowledges financial support from the Fondazione Ing. Aldo Gini.

REFERENCES

Baldry I. K., Balogh M. L., Bower R. G., Glazebrook K., Nichol R. C., Bamford S. P., Budavari T., 2006, MNRAS, 373, 469
Balogh M. L., Baldry I. K., Nichol R., Miller C., Bower R., Glazebrook K., 2004, ApJ, 615, L101
Bell E. F., de Jong R. S., 2001, ApJ, 550, 212
Berta S. et al., 2006, A&A, 451, 881
Bolzonella M., Miralles J.-M., Pelló R., 2000, A&A, 363, 476
Bolzonella M. et al., 2010, A&A, 524, A76
Brunner R. J., Lubin L. M., 2000, AJ, 120, 2851
Bruzual G., Charlot S., 2003, MNRAS, 344, 1000
Bundy K. et al., 2006, ApJ, 651, 120
Calvi R., Poggianti B. M., Fasano G., Vulcani B., 2011, preprint (arXiv:1110.0802)
Calvi R., Poggianti B. M., Vulcani B., 2011, MNRAS, 416, 727
Cava A. et al., 2009, A&A, 495, 707
Colbert J. W., Mulchaey J. S., Zabludoff A. I., 2001, AJ, 121, 808
Colless M. et al., 2001, MNRAS, 328, 1039
De Lucia G. et al., 2004, ApJ, 610, L77
De Lucia G. et al., 2007, MNRAS, 374, 809
Dressler A., 1980, ApJ, 236, 351
Ebeling H., Voges W., Bohringer H., Edge A. C., Huchra J. P., Briel U. G., 1996, MNRAS, 281, 799
Ebeling H., Edge A. C., Bohringer H., Allen S. W., Crawford C. S., Fabian A. C., Voges W., Huchra J. P., 1998, MNRAS, 301, 881

Ebeling H., Edge A. C., Allen S. W., Crawford C. S., Fabian A. C., Huchra J. P., 2000, MNRAS, 318, 333
Ellison S. L., Simard L., Cowan N. B., Baldry I. K., Patton D. R., McConnachie A. W., 2009, MNRAS, 396, 1257
Fasano G. et al., 2006, A&A, 445, 805
Gehrels N., 1986, ApJ, 303, 336
Gladders M. D., Yee H. K. C., 2000, AJ, 120, 2148
Gonzalez A. H., Zaritsky D., Dalcanton J. J., Nelson A., 2001, ApJS, 137, 117
Grützbauch R., Conselice C. J., Varela J., Bundy K., Cooper M. C., Skibba R., Willmer C. N. A., 2011a, MNRAS, 411, 929
Grützbauch R., Chuter R. W., Conselice C. J., Bauer A. E., Bluck A. F. L., Buitrago F., Mortlock A., 2011b, MNRAS, 412, 2361
Gunawardhana M. L. P. et al., 2011, MNRAS, 415, 1647
Haas M. R., Schaye J., Jeeson-Daniel A., 2012, MNRAS, 419, 2133
Halliday C. et al., 2004, A&A, 427, 397
Kauffmann G., White S. D. M., Heckman T. M., Ménard B., Brinchmann J., Charlot S., Tremonti C., Brinkmann J., 2004, MNRAS, 353, 713
Kroupa P., 2001, MNRAS, 322, 231
Liske J., Lemon D. J., Driver S. P., Cross N. J. G., Couch W. J., 2003, MNRAS, 344, 307
Maraston C., 2005, MNRAS, 362, 799
Martínez H. J., Coenda V., Muriel H., 2008, MNRAS, 391, 585
Milvang-Jensen B. et al., 2008, A&A, 482, 419
Moresco M. et al., 2010, A&A, 524, A67
Mouhcine M., Baldry I. K., Bamford S. P., 2007, MNRAS, 382, 801
Muldrew S. I. et al., 2011, preprint (arXiv:1109.6328)
Pelló R. et al., 2009, A&A, 508, 1173
Peng Y.-J. et al., 2010, ApJ, 721, 193
Poggianti B. M. et al., 2008, ApJ, 684, 888
Poggianti B. M. et al., 2009, ApJ, 697, L137
Roberts S., Davies J., Sabatini S., Auld R., Smith R., 2007, MNRAS, 379, 1053
Rudnick G. et al., 2001, AJ, 122, 2205
Rudnick G. et al., 2003, ApJ, 599, 847
Rudnick G. et al., 2009, ApJ, 700, 1559
Scodeggio M. et al., 2009, A&A, 501, 21
Scoville N. et al., 2007, ApJS, 172, 1
Taylor E. N. et al., 2009, ApJS, 183, 295
Valentinuzzi T. et al., 2009, A&A, 501, 851
Valentinuzzi T. et al., 2011, preprint (arXiv:1109.4011)
van der Wel A., 2008, ApJ, 675, L13
Varela J. et al., 2009, A&A, 497, 667
Vulcani B., Poggianti B. M., Finn R. A., Rudnick G., Desai V., Bamford S., 2010, ApJ, 710, L1
Vulcani B. et al., 2011a, MNRAS, 412, 246
Vulcani B. et al., 2011b, A&A, submitted
White S. D. M. et al., 2005, A&A, 444, 365
Wolf C. et al., 2009, MNRAS, 393, 1302
York D. G. et al., 2000, AJ, 120, 1579

This paper has been typeset from a TEX/LATEX file prepared by the author.